Dynamic modeling of natural gas quality within transport pipelines in presence of hydrogen injections

Giulio Guandalini *, Paolo Colbertaldo, Stefano Campanari

Politecnico di Milano, Energy Department, via Lambruschini 4A, 20156 Milano, Italy

In the near future, the natural gas grid could face an increasing share of alternative fuels (biomethane, hydrogen) injected in addition to the traditional mixture. Indeed, this pathway is particularly promising in order to reach environmental objectives of CO_2 emissions reduction, in both thermal and electrical final uses. Biogas is already abundantly produced and could be easily upgraded to biomethane; hydrogen technologies are still under development, but they can help the exploitation of the increasing availability of renewable energy sources. A promising solution to problems due to unpredictable fluctuations of renewable energy production (in particular related to wind parks) or excess energy with respect to the load lies in hydrogen production by electrolysis and further injection in the natural gas grid. In this scenario, the effects on design and management of the transport infrastructure should be investigated, and the compliance with composition limits and quality constraints has to be analyzed in both stationary and dynamic operation, tracking the gas quality downstream the injection point of the alternative fuels. A model was developed to simulate the unsteady operation of a portion of the gas grid; with respect to traditional volume-based approaches, a novel energy-based approach is developed, including variable com-position along the pipes and allowing to consider a given energy delivery to customers as a constraint. After the validation against available operational data, a case study considering concentrated realistic domestic and industrial offtakes is simulated. The effects of hydrogen injection, usually not considered in NG grid design and operation analyses, are investigated in terms of composition, flow rate and pressure profiles with comparison to the reference natural gas case. The analysis shows how imposed quality thresholds can be respected, although the effects on calorific value, Wobbe index and density are not neg-ligible; results indicate that the allowed hydrogen fractions are limited and highly sensitive to the profile and size of the offtakes connected to the pipeline. The discussion also evidences the potential impact of hydrogen injection on gas metering and measurements errors.

Keywords:Natural gas grid, Dynamic modeling, Alternative fuels, Hydrogen, Quality tracking

Highlights

Alternative energy-based approach for natural gas grid modeling.
Dynamic modeling of pressure and flows according to customer requirements.
Local composition calculation and gas quality tracking performed.
Analysis of delivered gas properties after hydrogen injection in a single pipe (case study).

1. Introduction

In the current energy scenario the share of renewables is expected to increase continuously, with respect to both fuels and electricity, also as a result of progressively stricter environmental policies [1–3] and general concern for emissions reduction. Biogas production can contribute significantly and the injection in the natural gas grid, after the upgrading process (e.g. the production of biomethane), is one of the most suitable pathway for valuing it [4,5]. With respect to traditional use of biogas for local cogeneration, the injection of 'green' gas in the grid improves also the environmental performances of distributed final users (i.e. domestic heating, industrial heat production). The majority of current biogas

Article history:
Received 31 August 2015
Received in revised form 26 February 2016
Accepted 2 March 2016
Available online 24 March 2016

---

* Corresponding author. Tel.: +39 02 2399 3935.
E-mail address: giulio.guandalini@polimi.it (G. Guandalini).

Published Journal Article available at: http://dx.doi.org/10.1016/j.apenergy.2016.03.006

Nomenclature

d	relative density to air (–)
D	pipe diameter (m)
ε	surface roughness (m)
$\dot{E}$	HHV energy flow (MJ/s)
Υ	hydrogen/natural gas flow ratio (–)
g	gravitational acceleration (m/s^2)
h	elevation (m)
HHV	higher heating value (MJ/Sm^3)
λ	friction factor (–)
p	pressure (Pa)
ρ	gas density (kg/m^3)
ρ_0	air density (kg/m^3)
q	mass flow rate (kg/s)
$\widehat{R}$	mass specific gas constant (m^3 Pa/K/kg)
Re	Reynolds number (–)
RMSE	root mean square error (–)
S	pipe cross section (m^2)
t	time (s)
T	temperature (K)
u	gas velocity (m/s)
$\dot{V}$	volumetric gas flow rate (m^3/s)
W	molar mass (kg/kmol)
WI	Wobbe index (MJ/Sm^3)
x	spatial coordinate (m)
$\bar{x}$	molar fraction
z	compressibility factor
LNG	liquefied natural gas
NG	natural gas
ODE	ordinary differential equation
P2G	power-to-gas
PDE	partial differential equation
TSO	transmission system operator

Subscripts

A	absolute
el	electric
mix	mixture (hydrogen/natural gas)
ng	natural gas
R	relative
r	pseudo-critical reduced property

production is utilized for local renewable heat and power generation; in the future, the share of upgraded biogas injected in the grid could reach up to 10–20% of the total demand [6], although the evolution of the market is subject to uncertainties related to energy policy evolution. Objectives set by Germany and Netherlands, which are the two countries with the strongest biogas market in Europe, are to cover 7% and 2% respectively of the total natural gas demand by biomethane in 2020.

Moreover, among the different solutions proposed to deal with the unpredictability of some renewable energy sources (wind and solar), energy storage in chemical form is a suitable option [7]. In particular, hydrogen production by means of electrolysis (the so-called power-to-gas or P2G concept) seems a feasible solution in order to reduce issues due to capacity limits and balancing requirements for electricity transmission grid control in case of high wind and solar power share, as well as a solution to manage very large storage capacities (MW to GW scale) [8]. Although the best economical valorization of hydrogen would come from its direct use in pure form, e.g. for feeding fuel-cell vehicles, hydrogen injection in the natural gas grid is a mid-term solution that avoids the necessity of a strictly contemporaneous and parallel development of final uses for the distributed hydrogen and postpones the development of a dedicated infrastructure [9]. As a term of comparison, considering a current consumption of natural gas of about 80 billons Nm^3 per year (Italy, Germany, UK [10]), a fraction of 5%$_{\mathrm{vol}}$ of hydrogen in the natural gas grid infrastructure could potentially store about 20 TW h per year of electrical energy from renewables, i.e. around 60–70% of the yearly production from wind and solar (Italy, [11]).

According to this picture, the management of the natural gas grid infrastructure will experience strong changes in the next future. In particular, the traditional assumption of limited variations in gas composition, typical of classic NG distribution scenarios, will not be valid anymore; the grid could start receiving several different gases, whose properties variations (heating value, density) could significantly influence the management of the grid. On the other hand, in most countries the regulation authorities are requiring more and more accuracy in the control of the gas quality delivered to the customers. Nowadays, first evidence of such issues are caused by the increasing diversification of gas sources, aiming at strategical safety of supply, which includes both pipeline connections to different production fields and a wider use of regasification of LNG coming from multiple countries. The addition of biomethane injections and, lately, of hydrogen injections will substantially increase the problem complexity. Therefore, the development of quality tracking tools in complex gas transport infrastructures is a urgent need.

Several models were developed in last decades [12], mainly aiming at optimal design of large-scale gas transport infrastructure; recently, an effort in modeling the dynamic behavior of the natural gas grid addressed the issue of pressure fluctuations due to an irregular usage of natural gas-fired power plants in presence of highly variable production from wind [13]. In literature, both stationary and dynamic analytical models are presented, with several dedicated solution methods dealing with the particular structure of the PDEs involved; nevertheless, they usually assume a constant composition of the gas mixture. An improvement is therefore required in order to properly take into account the presence of multiple sources of different kind of natural or synthetic gases. Literature models can be classified according to the solution approach. Key choice is whether or not enter the field of automatic control systems. In the first case, authors aim at extracting basic information about the behavior of the pipeline system – mainly for operation control purposes – by looking at the characteristics of the transfer functions obtained by applying a Laplace transform, after discretization and linearization of the analytical model [14,15]. On the opposite side, numerical solution of the two central PDEs of the model (continuity and momentum conservation equations) is sought with various levels of simplification [16–18]. An additional alternative exploits the electrical analogy, which leads to a less complex set of first-order ODEs [19].

In this work, a dynamic model is proposed that avoids the assumption of constant composition by evaluating the mixing of gas flows within any spatial interval at each time step. Moreover, since the energy content of the new blends of fuel gas delivered to the customers cannot be evaluated in simple terms of consumed volumes (as per the traditional gas metering approach), the model adopts energy-based boundary conditions to respect customers' requirements of a given energy delivery. After the model description, a validation of the approach is performed by means of comparisons with operational data from existing pipelines. Finally, a case study considering injection of pure hydrogen in the transport grid is analyzed; effects on grid operation are still not well known and much research effort is spent in assessing feasibility of this solution.

2. Model description

Unsteady gas dynamics in a pipe is governed by Euler equations for compressible fluids:

$$\begin{cases} \frac{\partial \rho}{\partial t} + \frac{\partial (\rho u)}{\partial x} = 0 \\ \frac{\partial (\rho u)}{\partial t} + \frac{\partial (\rho u^2)}{\partial x} + \frac{\partial p}{\partial x} + \rho g \frac{\partial h}{\partial x} + \lambda \rho \frac{u|u|}{2D} = 0 \end{cases} \quad (1)$$

written under the assumption of isothermal flow. The first equation is the conservation of mass, while the second is the momentum balance; energy conservation equation is substituted by the isothermal assumption. The assumption of constant temperature of the transported gas is considered valid in most cases; more generally, the comparison among the assumptions of isothermal conditions, adiabatic conditions or heat exchange with the environment (i.e. soil, depending on the geological features of the pipeline path) is discussed in literature. They mainly suggest a dependence on the scale of the problem, so that temperature effects are present and become significant when considering large scale infrastructures involving compression stations and pressure reduction devices as well as seasonal effects for soil temperature etc. [17].

Energy losses due to turbulence and wall friction are modeled through the last term of momentum balance in Eq. (1), according to Darcy–Weisbach formulation. Several approaches are available to relate the friction factor λ to fluid dynamics and geometries (Reynolds number *Re* and relative surface roughness ε/D). The implicit Colebrook–White model is the most complete and accurate [20], but it requires a dedicated solution step integrated in the global fluid dynamics solver; therefore, in this work, an explicit approximation is preferred. In particular, the Hofer formula [21], presented in Eq. (2), is applied.

$$\lambda = \left[2\log_{10}\left(\frac{4.518}{Re} \log_{10}\frac{Re}{7} + \frac{\varepsilon}{3.71D} \right) \right]^{-2} \quad (2)$$

An equation of state is mandatory to close the analytical problem, due to the compressible nature of the gas mixture; real gas behavior has to be considered due to the typical high pressures of the gas transport infrastructure. The deviation from ideal gas law is modeled through the compressibility factor z, as shown in Eq. (3).

$$p = \rho z \widehat{R} T \quad (3)$$

Composition influences both the specific mass gas constant $\widehat{R}$ and the compressibility factor; pressure and temperature dependence of the latter must be included, too. Several models can describe the volumetric behavior of gas mixtures with different accuracy; the most general formulations are based on two or three parameters equations of state with mixing rules (i.e. Redlich–Kwong). In the field of natural gas transport many correlations were developed in the past in order to simplify pipelines design, with sufficiently high accuracy in a specific range of pressure and temperature. Among them, the Papay formula (Eq. (4), [20]) takes into account the dependence on composition for pressures up to 150 bar, with deviations from more complex model smaller than 1.5% at 50 bar. Papay formula is:

$$z(T, p, \bar{x}) = 1 - 3.52 p_r e^{-2.260 T_r} + 0.274 p_r^2 e^{-1.87 T_r} \quad (4)$$

where p_r and T_r are the pseudo-critical reduced pressure and temperature of the mixture. Other models with much wider ranges of validity are the ISO standard model AGA8-DC92 and the GERG-2004 model [22,23], that are for instance implemented in specific codes as Refprop (by NIST) [24], used later in this work as benchmark and thermodynamic data calculator.

The approximation given by Eq. (4) does not affect the accuracy of the results when the considered fluid is natural gas, even with variable composition (from $80\%_{vol}$ to $99\%_{vol}$ methane content); therefore, it is used in this work for the model validation, Section 3, due to its low impact on the total computational time. However, in presence of uncommon species, it could affect accuracy, hence, the values of z in Section 4 are calculated through more complex and accurate equations of state (ISO models in Refprop libraries).

2.1. Energy-based approach and gas quality parameters

The traditional management of the grid is based on volumetric flow measurements, given that they offer an appropriate indication of what is transported and delivered to the customers (a pretty analogue situation holds for instance for gasoline or other liquid fuel delivery to customers). The presence of a time-dependent composition of the gas naturally leads to a different formulation of boundary conditions. We assume that final user consumption profiles are based on delivered energy and not on delivered mass nor volumetric flow, in order to maintain stable heat generation and operating temperatures in all the combustion devices connected to the grid. This approach is indeed currently adopted for the economic valorization of the natural gas, but not for grid management. In case of fluctuating compositions, physical flows should be real-time adjusted in order to deliver the required amount of energy.

An energy flow $\dot{E}$ [MJ/s] is defined as a function of volumetric flow rate $\dot{V}$ [m^3/s] and higher heating value HHV [MJ/m^3]:

$$\dot{E} = \dot{V} \cdot \mathrm{HHV} \quad (5)$$

The other fundamental quantities in Eq. (1) can be rewritten accordingly. In particular, velocity u can be rewritten as:

$$u = \frac{q}{\rho S} = \frac{\dot{E}}{\mathrm{HHV}} \frac{z \widehat{R} T}{p S} \quad (6)$$

where higher heating value HHV and compressibility factor z are functions of the local composition and, therefore, of the solution of the quality tracking problem itself.

From the point of view of the customers served by the transmission grid, the main indexes usually considered are the heating value HHV and the Wobbe index WI, defined as:

$$\mathrm{WI} = \frac{\mathrm{HHV}}{\sqrt{\rho/\rho_0}} \quad (7)$$

where ρ and ρ_0 are respectively the density of fuel gas and air at the same reference conditions. This is the main indicator of the interchangeability of fuel gases and its allowed range is specified by gas supply and transport utilities following country-specific rules and international grid standards. If WI for two gases of different composition is equal, then the energy output of the two gases is the same for a given pressure and using the same valve setting in the final apparatus (e.g. combustion system). The WI range defined by grid codes limits the fluctuation of composition that can be allowed without requiring technical interventions on the devices connected to the grid. Therefore, this index is particularly important for the application investigated in this work.

2.2. Solution of the discrete problem

The problem resulting from the previously described model has no algebraic solution and must be solved numerically. Here, we

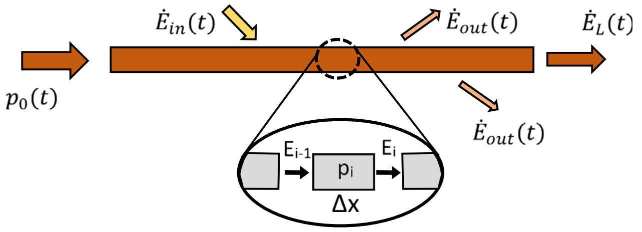

Fig. 1. Example of pipeline structure and required boundary conditions; detail of the applied spatial discretization scheme.

choose a finite volume approach: the pipe is discretized in a given number of volumes in which fluid properties are assumed constant (i.e. pressure, density, composition). Instead, flows are defined at the interfaces, as shown in Fig. 1. The figure gives also an example of the general structure of the simulated pipeline and of the required boundary conditions. Pressure is given at inlet because of the usual presence of a pressure-controlled system upstream (i.e. compression station, pressure reduction valve, larger pipeline). A number of offtakes subject to grid characteristics can be defined and for each of them a time-dependent energy profile must be set.

Combining Eqs. (1) and (3), considering as independent variables the energy flow $\dot{E}$ and the pressure p according to Eq. (6) (defined in discrete points as described above), the mathematical problem is summarized by the system of equations in Eq. (8), which has to be applied to each cell of the discretized domain. In addition, we consider here the hypothesis of horizontal pipelines so that the inclination term reduces to zero. However, the contribution of this term does not influence the general conclusions of this work due to its low magnitude.

$$\begin{cases} \frac{\partial p}{\partial t} = -\alpha \Delta \dot{E} \\ \frac{\partial \dot{E}}{\partial t} = -2\alpha \frac{\dot{E}}{p} \Delta \dot{E} + \left(\alpha \frac{\dot{E}^2}{p^2} - \beta\right) \Delta p - \gamma \frac{\dot{E}|\dot{E}|}{p} \end{cases} \tag{8}$$

$$\alpha = \frac{z\widehat{R}T}{S\Delta x} \quad \beta = \frac{S}{\Delta x} \quad \gamma = \lambda \frac{z\widehat{R}T}{2SD}$$

Initial and boundary conditions complete this stiff ODE problem. In particular, a complete profile of pressure p and energy flow $\dot{E}$ along the pipeline must be provided at $t = t_0$, together with the boundary conditions for each following time step.

The system is solved by the stiff ODE solver functions of MATLAB®; in particular, we use *ode15s* solver that is a variable order multistep algorithm based on the numerical differentiation formulas (NDFs) [25]. In each cell the effect on composition due to gas flow and possible local injections must be considered; an additional iterative procedure is set up, which calculates the composition according to mixing rules and updates related coefficients in each cell within ODE algorithm iterations.

The spatial discretization must be defined in advance; $\Delta x = 200$ m is assumed and the influence of different values verified, yielding no significant differences. Smaller values could improve the accuracy, but bring about numerical instability as there is a relation with the time discretization, which is determined by the ODE solver at each step. Too small spatial intervals prevent from obtaining a solution because the pressure waves considered by the simulation pass through more than one cell in a single time step, making it impossible for the algorithm to calculate the values in between.

As in any unsteady problem, the choice of a correct initial condition strongly influences the quality of the results; in this work the steady state solution at $t = t_0$ for the given boundary conditions is used to give initial values of pressure and flows in each cell; uniform composition of the gas along the pipe at $t = t_0$ is also assumed. This approximation may yield unreliable results for an initial period of the simulation, whose duration has to be estimated case by case. Due to the common operation of natural gas pipelines, in which the gas flows in the same direction for long periods, it is reasonable to assume that after a certain amount of time all the initial 'unknown gas' inside the pipeline will be substituted by the injected one, whose characteristics are known. Observation of the results will then be valid only after that initial period, whose duration depends on pipeline size and flows. For the validation carried out in Section 3, the initial period lasts about 10 h, compared to a total simulation period of one week.

3. Validation against grid data

In order to verify the functioning of the model, a validation is performed by comparing the results to a benchmark simulation. The latter comes from the software currently used by the Italian TSO of the national natural gas grid (SIMONE [26,27]), based on real operational data. A grid portion is suitable for the purpose if the natural gas flows with a predefined unique direction and the boundary conditions (as described in Section 2.2) are known.

A case involving real linear pipes of the Italian national grid, located in central Italy, is evaluated. The nominal maximum pressure is 75 bar_g and the length is about 60 km; nominal diameter is 900 mm in the first half and 600 mm in the remaining. Four offtakes are included, distributed along the whole pipeline. No intermediate injections are present, while boundary conditions (inlet pressure, inlet composition, outlet energy flow and energy flows at offtakes) are assigned as function of time (hourly base). The simulation consists of 168 h of operation, equal to one week.

In order to understand the actual potential of the simulation, differences from benchmark values are evaluated through the error indicators defined in Eq. (9).

$$\begin{aligned} E_A &= \text{HHV}_{simulation} - \text{HHV}_{benchmark} \\ E_R &= \frac{\text{HHV}_{simulation} - \text{HHV}_{benchmark}}{\text{HHV}_{benchmark}} \\ \text{RMSE}_{A,R} &= \sqrt{\frac{1}{n}\sum 1nE_{A,R}^2} \end{aligned} \tag{9}$$

The profile of the simulated HHV in significant points of the pipeline is shown in Fig. 2 together with the values from the benchmark simulation. Fig. 2c also includes the field measurements as further comparison. The wide variation of the values along the time demonstrates that a real variation of composition is considered, including daily or hourly peaks. Beyond punctual differences of the values, a good reconstruction of the profile is visible. A significant gap is present only in the initial period of the simulation; this difference is related to the assumptions on the characteristics (composition and therefore HHV) of the natural gas present at the starting moment. A uniform composition is supposed to fill the whole pipeline, instead of the real one that depends on the characteristics of the natural gas flown during the previous period. However, due to the flow conditions, the natural gas in the pipe is totally consumed within a short amount of time, which depends on the physical characteristics of the pipeline and on the offtakes. The time span of inaccurate HHV reconstruction differs along the pipeline; in particular, the positions $x = 11$ km, $x = 37$ km and outlet are shown in Fig. 2. In order to keep this 'initialization' effect out of the evaluation, the first day of simulation is neglected from error calculation, since it is influenced by the assumption of composition homogeneity along the pipeline at the initial moment more than by physical inaccuracy of the model. From the simulation setup point of view, an additional initial period of simulation must be included before the time span of interest.

A common feature of the simulated profiles is a slight underestimation of the HHV, almost constant in the whole period

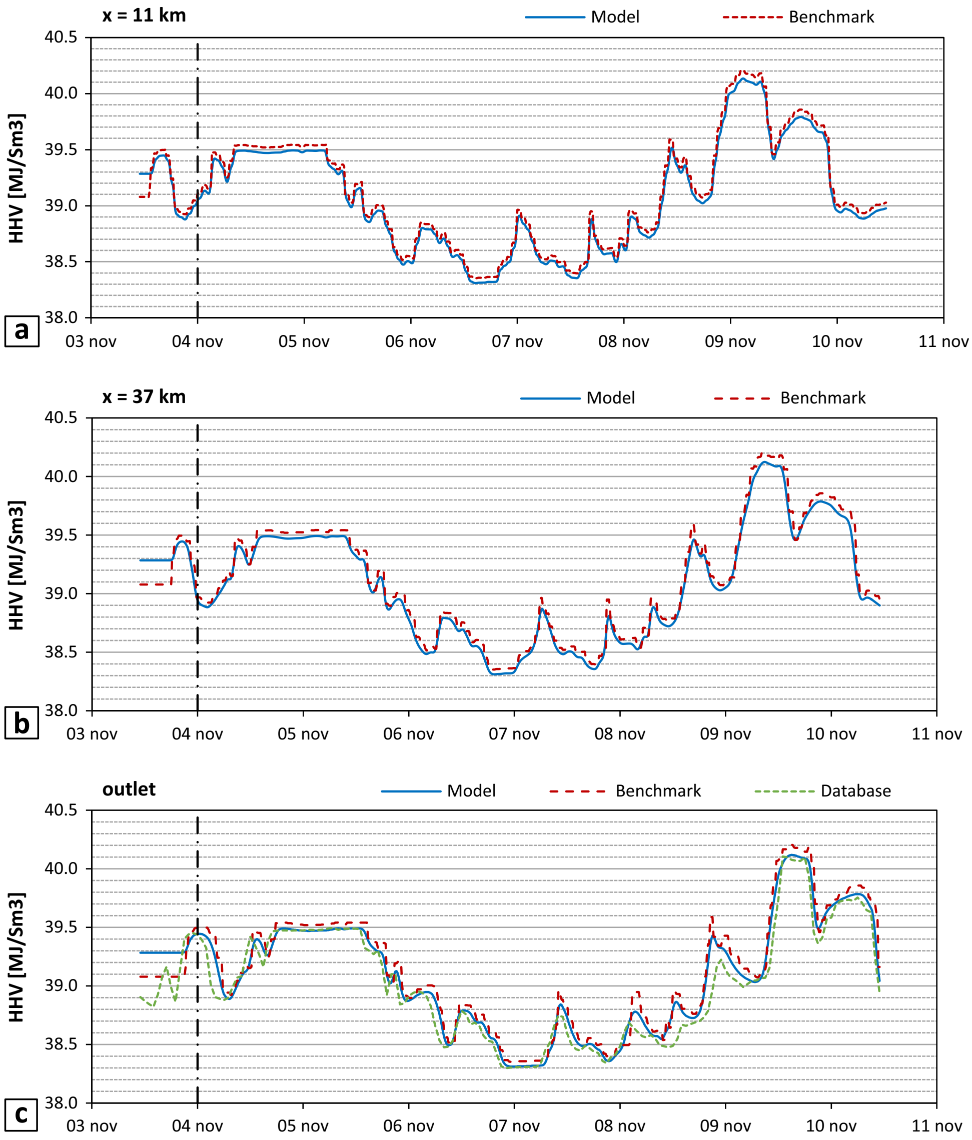

Fig. 2. Profiles of higher heating value resulting from the simulation, compared to the benchmark ones and to the database values (when available): (a) at the first offtake ($x = 11$ km), (b) at the third offtake ($x = 37$ km), (c) at the outlet ($x = 60$ km).

Table 1
Absolute and relative errors in HHV estimates between model and benchmark.

Offtake position		11 km	31 km	37 km	49 km	Outlet
E_A max	MJ/Sm^3	0.079	0.066	0.119	0.115	0.199
E_A min	MJ/Sm^3	−0.188	−0.305	−0.324	−0.340	−0.412
RMSE$_A$	MJ/Sm^3	0.056	0.065	0.068	0.073	0.079
E_R max	%	±0.48%	±0.77%	±0.82%	±0.86%	±1.04%
RMSE$_R$	%	0.14%	0.16%	0.17%	0.18%	0.20%

considered. This is most probably due to the use of different reference databases for the species thermo-physical characteristics. Moreover, a relevant aspect is the different shape of peaks, clearly visible between Fig. 2b and c; this effect shows that the model provides a correct fluid-dynamic reconstruction of the flow and not only a time shift of the profile. In Fig. 2c a particular situation occurs: on November 8th both the model and the benchmark overestimate quite significantly the HHV, showing peaks that are not reached in practice (database values). Comparison must however take into account that not only the model has approximations, but also the measurement system is affected by uncertainties.

The values of the errors are summarized in Table 1. Higher values are reached as the distance from inlet increases. Looking back at Fig. 2, a limited horizontal translation can be noticed in cases b and c, corresponding to positions located after the change of pipeline diameter. A possible explanation is a different localized pressure loss at the shrinkage section, causing a discrepancy in velocity estimation in the second half of the pipe. However, the maximum relative error does not exceed 1% and RMSE$_R$ is largely lower than 0.5%; as a reference, the current maximum accepted HHV difference among homogeneous areas is 2% for the Italian TSO rules and methodology.

4. Hydrogen injection case study

As mentioned in Section 1, injections of non-conventional gases in the natural gas grid infrastructure are possible and supported by environmental policies. Biomethane injection influences gas properties, but in practice it is not so different (apart from the cases of non-conformity due to incorrect upgrading) from a high-methane content natural gas; the long-term option of hydrogen injection offers more challenges in terms of impact on grid operation and on customers. Indeed, hydrogen volumetric, thermal and chemical properties strongly differ from the ones of the species in typical natural gas. In this work, we consider as case study the injection of hydrogen in an existing medium-pressure pipeline of the Italian natural gas transport infrastructure, in order to assess the impact on the gas delivered to customers.

A dynamic modeling of the system is mandatory, due to the time dependent flow in the pipeline and to the variability of hydrogen production, which is based on the abovementioned P2G technology, thus related to the availability of excess energy from the renewable source upstream.

Hydrogen admixture in natural gas grid is already in practice in a few demonstrative plants in Germany and scheduled in UK [28–31]. Some limitations to hydrogen volumetric fraction in the final mixture are imposed according to several studies [32,33]. These limits are currently set to 5%, but hydrogen fractions up to 10–20% are addressed as safe for most applications. Nevertheless, this limit must be combined with current limitations on heating value and Wobbe index allowed for injections in natural gas grid, in order to consider the most restrictive one; mixture properties and composition can be calculated according to Eqs. (10)–(12). The final volumetric fraction of hydrogen can be calculated from

$$x_{H2}^{mix} = \frac{\Upsilon + x_{H2}^{ng}}{1+\Upsilon} \tag{10}$$

where Υ is the ratio between molar flows of hydrogen and natural gas before admixture; the hydrogen fraction in natural gas x_{H2}^{ng} is usually negligible. Volumetric higher heating value of the mixture is lowered by hydrogen injection ($HHV_{H2} = 12.09$ MJ/Sm^3) according to:

$$HHV_{mix} = \frac{\Upsilon \cdot HHV_{H2} + HHV_{ng}}{1+\Upsilon} \tag{11}$$

On the other hand, Wobbe index of the mixture depends on several parameters:

$$WI_{mix} = \frac{HHV_{mix}}{\sqrt{d_{ng} \cdot \frac{1+\Upsilon \cdot \frac{W_{H2}}{d_{ng} \cdot W_{air}}}{1+\Upsilon}}} \tag{12}$$

where d is the relative density to air at standard conditions (15 °C and 1 atm) [22] and W are the molecular weights of hydrogen and air. This approximation is valid under the assumption that the ratio between the compressibility factor of air and natural gas is one, reasonable at reference conditions.

The combined effect of the previously discussed limitations is depicted in Fig. 3. The maximum allowed volumetric fraction of hydrogen in the mixture (x_{H2}^{mix}) is given as a function of heating value and Wobbe index of the inlet natural gas; current limits in Italian TSO grid code [34] are evidenced as dotted lines. As expected, the lower the initial heating value of the gas, the lower the admissible hydrogen fraction; horizontal limits are instead related to modifications in Wobbe index. As basis for comparison, five standard gases commonly transported in the European system are represented, classified accordingly to their origin. Despite the various properties, all of them are in the central region of the chart and allow adding volumetric fractions of hydrogen up to 10% without crossing the given thresholds; consequently, in the following the most restrictive limit on hydrogen fraction is assumed for defining the injection profiles.

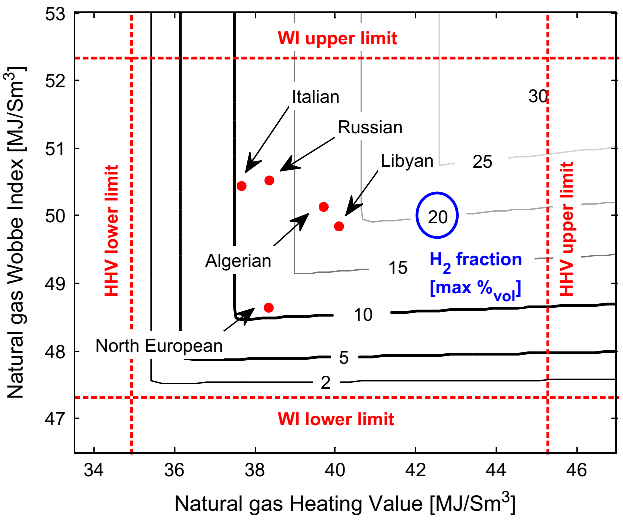

Fig. 3. Maximum allowed hydrogen volumetric fraction (%) in order to fulfill TSO requirements (dotted lines; values referred to Italy limits) as function of natural gas properties (HHV and WI); some NG types commonly present in the European grid are located as reference.

The pipeline chosen for the simulation has a diameter of about 600 mm (24 in.) and a nominal pressure of 50 bar, being part of the regional transport system; a 50 km section of pipe is considered in order to analyze the hydrogen injection effects. The structure of the offtakes is shown in Fig. 4, while an injection point is assumed at about one third of the pipe. The reference composition of natural gas considers a Russian gas (96.51% CH_4, 1.66% C_2H_6, 0.62% C_3H_8, 0.26% CO_2 and 0.79% N_2, HHV 38.28 MJ/Sm^3). Simulation horizon is limited to 48 h.

4.1. Injection and offtake profiles

Injection and gas extraction profiles are particularly important in this analysis due to their influence on fluctuations of gas properties perceived by the customers.

The reference natural gas flow (about 42.2 kg/s, 215 kSm^3/h) in the original pipeline is imposed at the outlet, considered as in transit to downstream customers; the assumption on calorific value of the reference natural gas yields an outlet energy flow of about 2274 MW_{HHV}. This profile corresponds to the one measured in a similar pipeline in Southern Italy in 2012 on a spring day. The inlet flow is therefore a consequence of intermediate offtakes and fluid dynamics.

Hydrogen input flow in this case study is calculated according to the most restrictive criteria (see Fig. 3); in particular, the $5\%_{vol}$ hydrogen fraction limiting condition is assumed considering a dummy mixing of the hydrogen and a natural gas flow whose energy content corresponds to the outlet flow at the same moment (hourly based). The injected flow depends on the combination of the fraction limit and the forecasted production profile calculated in a separate work for a P2G system connected to a wind farm, whose operation has been optimized according to the model described in [35]. Both natural gas and hydrogen profiles are shown in Fig. 5.

Hydrogen production is subject to fluctuations of the intermittent energy source; a buffer storage smooths the injection profile, but hydrogen flow depends on excess wind availability. A period with a large wind availability is chosen in order to maximize the

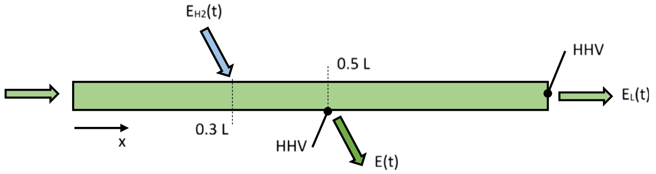

Fig. 4. Structure of injection and offtake points for the case study; gas properties (HHV and composition) are checked at the offtakes.

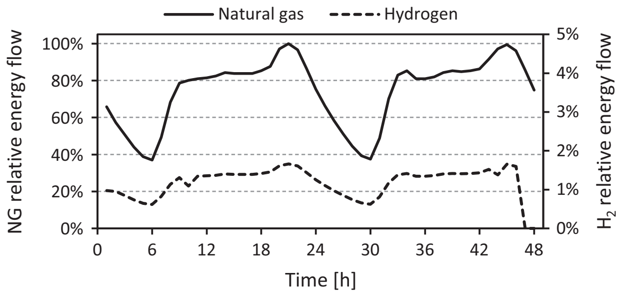

Fig. 5. Natural gas transit energy flow and hydrogen injection in a medium pressure pipeline, relative to the peak flow of NG (about 2274 MW_{HHV}, corresponding to 215 kSm^3/h).

effects of the admixture in natural gas grid; nevertheless, some small deviations from maximum are present (i.e. 8 and 43 h) and in the last hours the production is zero due to lack of wind and empty buffer. Thus, the analysis allows also to check the effects on the extraction points (and related customers) of a sudden comeback from the modified gas to a traditional natural gas composition.

With respect to the gas extraction from the pipeline (offtakes), the demand strongly depends on the kind of customers connected to the grid. In order to develop an analysis that can be representative of a plausible and realistic situation, while remaining as general as possible, the contemporary presence of a residential and an industrial customer is considered. In particular, the profiles in Fig. 6 are adopted. A residential profile (including both domestic users and small firms) repeats itself in the two days, while an industrial profile is included in the first day, corresponding to a power plant (natural gas combined cycle, 400 MW_{el}) whose output decreases close to noon due to solar plants contribution to electricity production. The second day is assumed to be a weekend day during which the power plant is not operated.

Inlet pressure is set to 50 bar, according to the assumption that the pipeline is located downstream a compression station or a pressure reduction system and, therefore, not subject to fluctuations. This allows to check the influence of hydrogen injection on delivery pressure at offtakes.

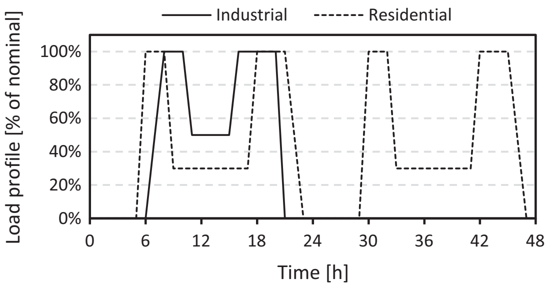

Fig. 6. Demand (load) profiles for the case study (nominal 910 MW_{HHV}).

4.2. Impact on fluid dynamics in the pipeline

A first analysis is dedicated to the dynamics inside the pipeline, which is investigated in terms of pressure drops, densities and velocities. Changes and oscillations of these values have an impact on grid management and their variation shows clearly the physical effect of small hydrogen fractions in natural gas. In order to understand the results, it is important to consider that the order of magnitude of sound velocity in this case is around 380 m/s. On first approximation, it means that a pressure variation goes through the whole pipeline (in this case, a 50 km section) in about 2 min, while mass flow is much slower and needs about 3–4 h to reach the outlet. This difference in travel time justifies the different dynamics, which will be evident in the following discussion.

Pressure drop profile is shown in Fig. 7a as function of time and space; fluctuations along the time depend on flow variations (imposed boundary conditions) and on gas properties modifications. In Fig. 7b the detail of the profile along the pipe is shown for some relevant time steps; the results of the case study are compared with a constant composition benchmark under the same boundary conditions of pressure and energy requirements. At time zero, the whole pipeline is filled with natural gas, the offtakes are null and the outlet flow is about 60% of the peak (see Figs. 5 and 6). At *t* = 8 h, both offtakes reach the peak, while the outlet is still at about 80% of the peak and the presence of hydrogen in the pipe is already relevant. At *t* = 20 h, the outlet flow reaches the maximum together with the offtakes. The final time step (*t* = 48 h) is also included because it follows a period of two hours without hydrogen injection (see Fig. 5); flow is low due to the absence of offtakes and the pipe is still partially filled with H_2–NG mixture, making this condition of interest from the point of view of the discussion.

Pressure drop depends mainly on the flows required by offtakes; the effect of the offtake at *x* = 25 km is evident in Fig. 7b, corresponding to a strong slope change. It turns out that the presence of hydrogen, at the stipulated fractions, has only very small effects on the pressure drop profile (with differences below 0.1% with respect to NG benchmark), since most of the variations are dictated by the gas extraction profiles. Due to that, the profiles for the H_2–NG mixture are almost coincident to the profiles for the reference natural gas. No spatial delays can be distinguished due to the high speed of pressure waves propagation.

The effect of hydrogen injection becomes much more significant on density profiles, which are depicted in Fig. 8 with the same criteria chosen for pressure drops. Two effects can be highlighted: (i) a sudden step in density is located at about one third of the total length, and is generated by the hydrogen injection; (ii) density fluctuations are visible at the outlet, where they are mostly generated by pressure drop variations. The extremely low density of hydrogen determines a significant variation in the mixture density even with the small quantity introduced. The step corresponds to about 4% of natural gas density in the reference case, and its impact would be significant both for pipeline management (influencing for instance the control and consumption of compression stations) and for customers at extraction points. Variations in the offtakes yield evident effects (corresponding to the ones in pressure profile) in terms of slope change, which are present also in the reference NG case. The density shows the delay in mass transport, as can be observed in Fig. 8b where the density change due to admixture during the first period is a function of the position. Moreover, the presence of hydrogen is still noticeable at *t* = 48 h in the final section of the pipe, even though the injection stopped two hours before.

The last quantity analyzed is the gas velocity, whose profiles are drawn in Fig. 9. Also in this case, the steps due to hydrogen injection and offtakes are evident. Density reduction and additional

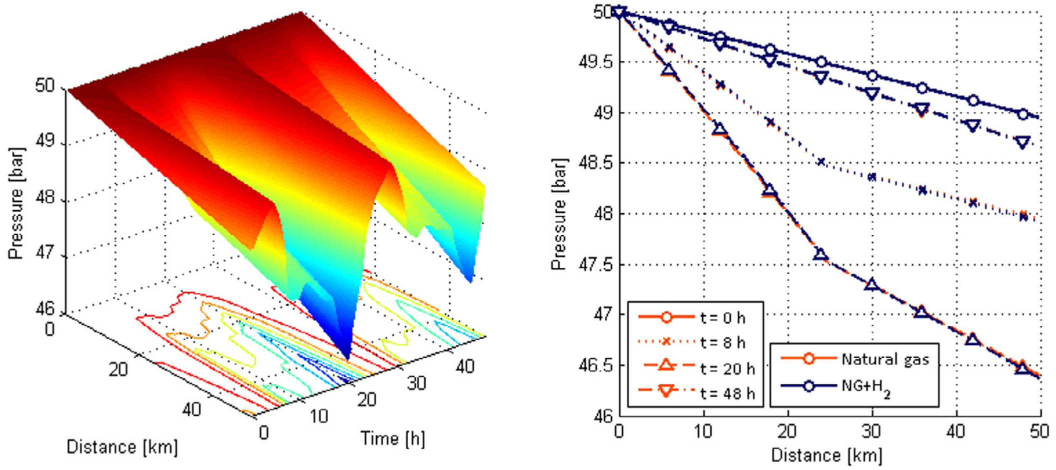

Fig. 7. Pressure profile as function of time and position for the case with hydrogen injection (left); comparison of profiles with and without hydrogen for some relevant time steps (right).

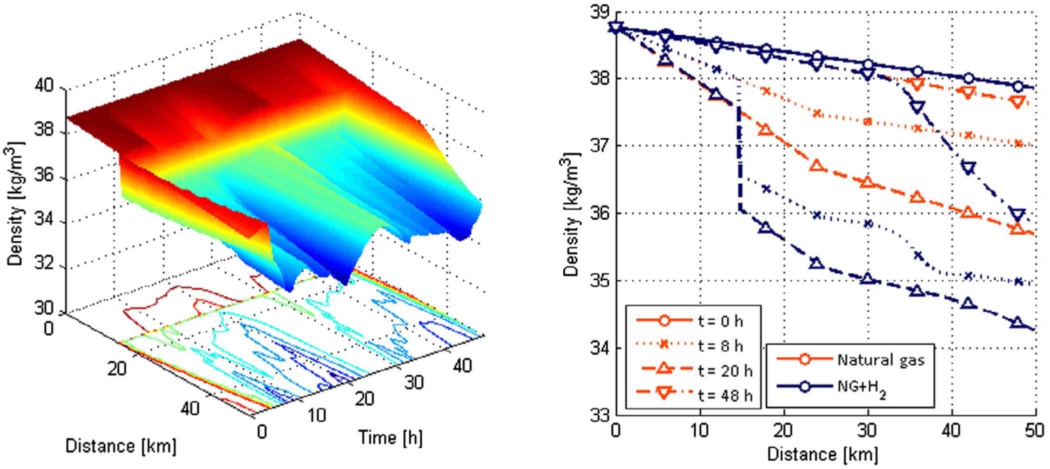

Fig. 8. Density profile as function of time and position for the case with hydrogen injection (left); comparison of profiles with and without hydrogen for some relevant time steps (right).

flow corresponding to the admixture of hydrogen cause a small increase of velocity; the strongest effect is however the flow reduction due to the large offtake in the middle of the pipeline. This contribution is approximately the same both for the mixture case and for the natural gas benchmark. Velocity variations due to the loads are important because they directly influence pressure drops, as can be observed comparing Figs. 9 and 7.

4.3. Gas composition and delivered energy

This section is dedicated to the analysis of hydrogen admixture impact on delivered gas composition and flows. Hydrogen molar fraction profiles at the offtake position and at the end of the pipe are shown in Fig. 10, with the profile of injected hydrogen as comparison. A time shift is clearly visible, showing that the injection profile and the related composition wave propagate along the pipe. The shape remains very similar, although there is a smoothing effect on the sharpest peaks and some changes are present in gradients and concavity of the profiles. Hydrogen content gradients are below 0.07%/min during periods of injection, but they reach values up to 0.3%/min in case of sudden startup.

The most sensible fluctuations in hydrogen fraction correspond to the period of large offtakes (i.e. industrial in the first day). As the hydrogen flow is calculated from the reference flow at the outlet, in presence of relevant extractions, the amplified flow upstream determines a dilution of the alternative gas in the mixture. On the opposite, the reduction or vanishing of a load causes peaks in hydrogen concentration. It appears that the highest peaks slightly exceed the $5\%_{\mathrm{vol}}$ limit (maximum equals to 5.1%). First, this fact underlines the importance of dynamic simulation methods in the investigation of such a technology. Second, the resulting behavior is related to the hypothesis used for the calculation of the hydrogen injection profile. In fact, the procedure gives the hydrogen flow that allows to respect the limit on hydrogen fraction downstream (set at $5\%_{\mathrm{vol}}$) by considering a dummy mixing between the hydrogen flow itself and a natural gas flow equivalent – as energy content – to the flow imposed at the outlet at the same moment (hourly based). Two effects can be noticed:

- in presence of high loads, the resulting overestimation of the hydrogen flow is counterbalanced by the increase in natural gas flow at the inlet, leading to low molar fractions downstream;

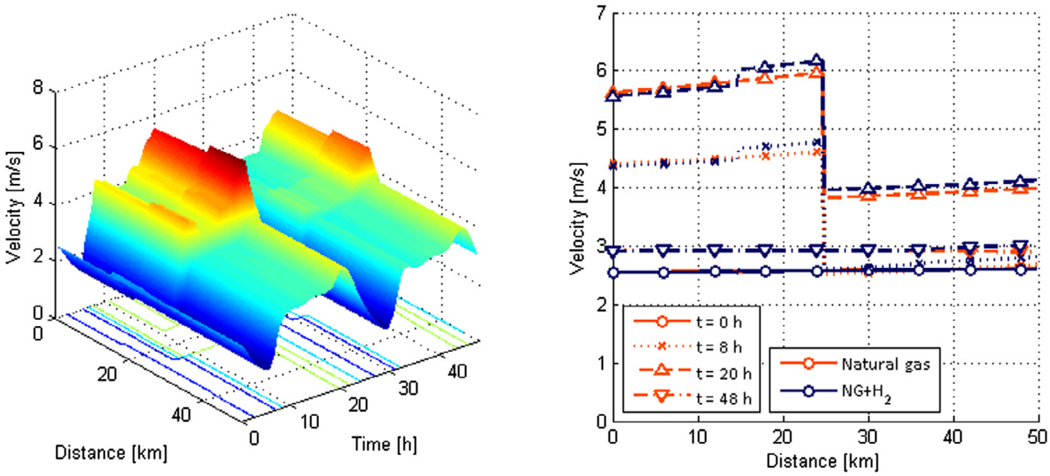

Fig. 9. Velocity profile as function of time and position for the case with hydrogen injection (left); comparison of profiles with and without hydrogen for some relevant time steps (right).

- on the opposite, during periods of decreasing flow at the outlet $\left(\frac{\partial \dot{E}}{\partial t} < 0\right)$ the actual natural gas flow upstream the injection is even smaller than the value considered for the hydrogen definition and therefore the limit could be exceeded (compare Figs. 5, 6 and 10).

A local evaluation of the exact maximum quantity of hydrogen allowed would keep molar fraction constantly below the limit. However, it is not considered both for numerical reasons (a simulation following this approach requires an extra nested cycle) and for its poor practical feasibility, requiring multiple flow measurements that are not likely to be repeated on single pipes in real applications.

As additional comparison, Fig. 11 shows the calculated hydrogen fraction along the pipeline. Initially, hydrogen fraction is null all along the pipe, while a step corresponding to the distance of 14 km evidences the injection point. Mass transport governed by convection generates a step shape profile where the front of gas having a different composition moves further. Depending on the position and time, the hydrogen fraction then changes remarkably between zero and the maximum. At the end of the investigated period ($t = 48$ h), injection was already stopped (set to zero at $t = 46$ h, see Fig. 5 for comparison), but the pipeline is still containing hydrogen for a long portion. The resulting profile evidences the delay (proportional to the flow rate) of the restored original NG composition in reaching the intermediate offtake and the pipeline outlet.

In Fig. 12 the higher heating value of the NG–H_2 mixture is compared to the one of natural gas at inlet. A reduction is evident, whose starting point is shifted in time as much as the position is distant from the injection. The shape is shifted horizontally depending on the position considered and it reflects the hydrogen volumetric fraction profile represented in Fig. 10. The HHV difference does not exceed 1.35 MJ/Sm^3.

As mentioned in Section 2.1, a fundamental parameter to check the acceptability of alternative gas injection in the grid is the Wobbe index. The resulting profile in the simulation performed is shown in Fig. 13. In the initial period, the mixture composition along the pipeline is uniform and no hydrogen is present; WI index at offtakes position and at outlet is slightly higher than at inlet due to the lower pressure (and consequent lower density), according to Eq. (7). In the following simulated period, the presence of hydrogen determines two effects: (i) increased compressibility factor and decreased molecular weight of the mixture, i.e. smaller density, leading to a WI increase proportional to its square root; (ii) reduced HHV of the mixture, causing a proportional reduction of WI. As the variation of the square root of density at denominator is overcome by the variation of the HHV at numerator, the effect of hydrogen in the mixture is a slight decrease of WI. The variation is, however, very limited (max 0.3 Sm^3/h), showing that hydrogen injection below $5\%_{vol}$ has a low impact on the connected combustion devices, although additional effects should be estimated.

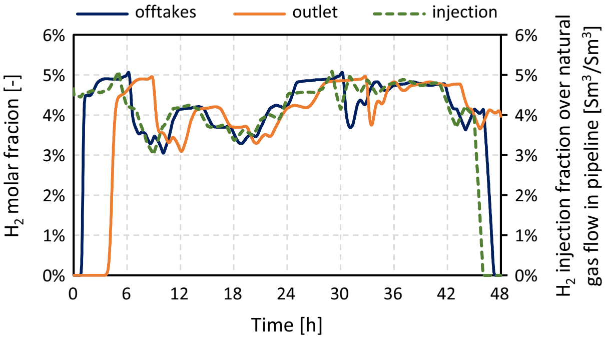

Fig. 10. Hydrogen volumetric fraction profile at offtakes (blue) and at outlet (red), referred to the left axis, compared to injected hydrogen flow (relative to the mixture flow just before the injection point, on volumetric basis; yellow), referred to the right axis. (For interpretation of the references to colour in this figure legend, the reader is referred to the web version of this article.)

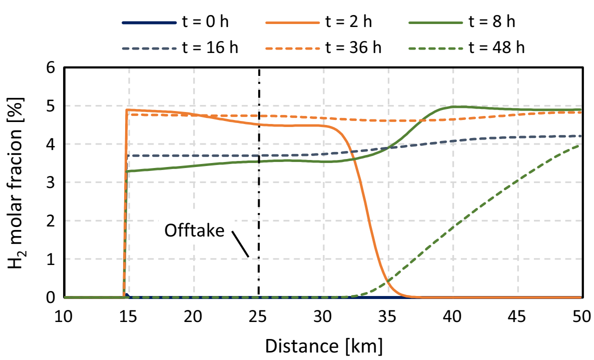

Fig. 11. Hydrogen volumetric fraction profile at different time steps as function of distance from inlet. Injection point is located at 14 km from inlet.

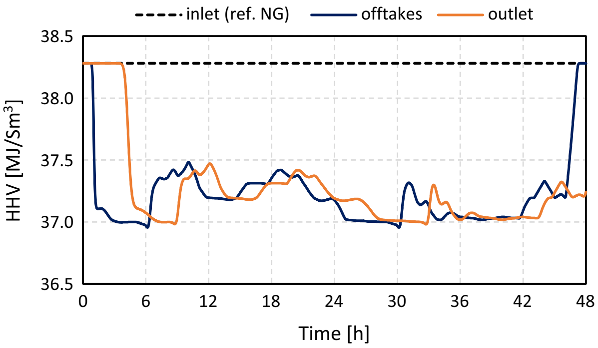

Fig. 12. HHV profile at offtakes position (blue) and at outlet (red), compared to the value at inlet (dotted black). (For interpretation of the references to colour in this figure legend, the reader is referred to the web version of this article.)

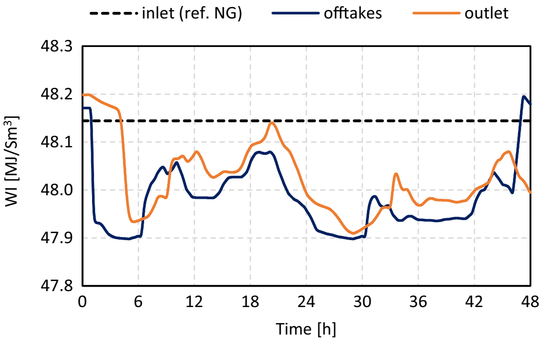

Fig. 13. Wobbe index profile at offtakes position (blue) and at outlet (red), compared to the value at inlet (dotted black). (For interpretation of the references to colour in this figure legend, the reader is referred to the web version of this article.)

The last analysis considers the effect of hydrogen injection on offtake variations, in terms of volumetric flow that the users need to set in order to obtain the same energy flow. The increase in required volumetric flow is evident in Fig. 14 for the residential offtake; during the peaks, the variation is around 2 kSm^3/h, equal to 3.8% of the original amount. Analogue considerations apply to the industrial user. Considering the H_2 molar fraction profile, it can be noticed that the hydrogen percentage decreases during high-load periods, due to the higher flows upstream.

Additional simulations have been performed, considering a different composition of the natural gas at inlet (typical Algerian NG, ethane- and propane-rich, or usual Italian NG, methane-rich) or a different hydrogen limit allowed in the mixture (up to 10%). In both cases, results are analogue to the ones presented above in terms of profile shapes and percentage differences, with molar fractions and HHV changes that are proportional to the variation of upper hydrogen injection limit. Higher hydrogen contents have not been considered because they would determine the exceeding of the current limitations imposed by the TSO already in stationary conditions (see Fig. 3).

4.4. Effects on gas metering

The presence of unexpected hydrogen fractions in the flowing mixture could affect the accuracy of the volumetric metering systems currently used for NG delivery measurements. In fact, the quantity of interest (volume flow rate at reference conditions, expressed as Sm^3/h) is obtained from the measured one (volume flow rate at operating conditions) through a post-processing of the data in which the composition plays a significant role.

In a volumetric meter, the measured values are the “units of volume” UC [m^3] (i = initial, f = final) that enter or exit the chamber of the measurement device in a specified time step (i.e. hour); the flowing volume V [Sm^3/h] is then obtained as:

$$V = (UC_f - UC_i)K \tag{13}$$

where K is a conversion coefficient defined as:

$$K = \frac{pT_S z_S}{p_S T z} \tag{14}$$

The subscript S in Eq. (14) indicates the conditions (typically ISO Standard: 1.01325 bar, 15 °C) at which the measure has to be referred. As most of the meters are not coupled with an instrument for the local evaluation of the composition, due to cost and reliability issues, the compressibility factor z in the formula cannot be accurately estimated. As long as the flowing mixture is a typical natural gas with limited variability of the composition, the evaluation of z can be performed from available historical data, for instance using the composition of the mixture in a reference period (e.g. two months before [34]). These data are usually available to the TSO, who measures them through specific instrumentation (e.g. gas chromatography) in key points of the NG grid. Keeping the current setting of the meters, at times during which hydrogen is present, a relevant error could occur, due to a significant change in the compressibility coefficient of the gas. This error would affect both the management of the grid and the accounting of the delivered natural gas, yielding significant errors in the billing procedures.

In order to assess the magnitude of the error, the value of K calculated with a reference natural gas composition is compared to the value of K based on a hydrogen-enriched composition. For a methane-rich (about $99\%_{vol}$) natural gas mixture, the volume calculated in presence of about $5\%_{vol}$ hydrogen is 1.3% higher than real at 50 bar and 0.5% higher at 24 bar. For a low-methane (about $85\%_{vol}$) natural gas mixture, the error increases up to 1.7% at 50 bar and 0.7% at 24 bar. By increasing the allowed hydrogen content to $10\%_{vol}$, the worst case (low-methane mixture at 50 bar)

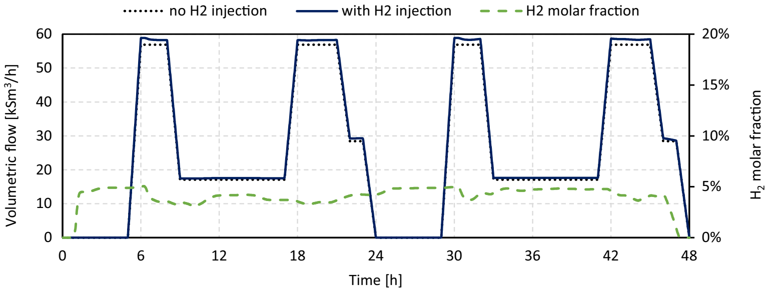

Fig. 14. Volumetric flow profile at residential offtake in case of presence (blue) or absence (dotted black) of hydrogen injection, together with HHV profile (green) at the same position. (For interpretation of the references to colour in this figure legend, the reader is referred to the web version of this article.)

shows an error in the flow rate evaluation over 3%. Due to the volumetric behavior of hydrogen, it can be noticed that the error increases with the pressure, thus affecting the industrial customers on the transport grid (e.g. large utilities, energy-intensive industries, power plants) more than the domestic deliveries on the distribution grid. Moreover, the inaccuracy grows with the increase in allowed hydrogen content. On the other hand, these maximum errors would represent the actual error in the flow rate evaluation only in periods during which hydrogen is continuously fed into the grid with quantities close to the maximum allowed, whereas lower discrepancies would occur in intermediate periods. Indeed, as the Power-to-Gas technology aims at exploiting excess renewable energy, an intermittent functioning of the electrolyzers which are generating hydrogen can be expected, leading to a discontinuous injection in the grid; thus globally, due to the variation – and even absence – of the hydrogen injection over long periods, the average error would be smaller than the maximum values presented above. At any rate, the correct evaluation of H_2 fraction along the grid appears to hold remarkable importance, evidencing the usefulness of appropriate prediction and simulation tools. To further assess the actual variations introduced in the flow rate measurement values, simulations on longer time step are required, taking into account appropriate hydrogen profiles as well as more complex grid topologies.

5. Conclusions

In this work, a model has been developed in order to simulate dynamic gas transport in pipelines, considering both variable local composition and an energy-based approach for boundary conditions. In this way, it is possible to model the injection of alternative fuels in the natural gas grid infrastructure, taking into account the influence they have on local properties of the gas. The choice of energy-based boundary conditions (instead of volume-based) helps the definition of realistic offtakes, reflecting the necessity to guarantee the customers' energy demand independently of the composition; with respect to traditional models, this requires a different iterative solution (mass inlet flow depends on composition that is an output of the model). The model, applied to a test pipe simulation, leads to errors in the order of 1% compared to benchmark simulation software and reference data, in terms of transported energy. The application of such a simulation tool would offer advantages to the TSO in the activities related to grid operation and planning, as well as to the customers in improving gas metering accuracy. First, an *ex-post* flow reconstruction could lead to an accurate accounting of the delivered energy, improving economics and billing procedures; second, *ex-ante* simulations would be beneficial to the design and positioning of new injection points, by taking into account the subsequent effects on the offtakes in terms of composition and HHV ramp rate.

The results of the test case simulation show that the influence of hydrogen injection, commonly considered a potentially strong perturbation on grid operation, leads to negligible effects on pressure drops (differences below 0.1%), whereas the density and the velocity of the fluid are influenced. An upper limit of 5% is chosen here for the simulation, according to current limits imposed in demonstrative projects. In practice, fractions over 10% already exceed TSO limits on HHV and WI (as seen in Fig. 3), even neglecting dynamic effects. The results of hydrogen injection case study show the importance of a dynamic analysis, evidencing H_2 molar fraction different from expected due to the dynamic fluctuations of the flow in the pipe.

Significant effects are evident on HHV and WI, which change respectively by 3.5% and 0.6%. Although the values remain in the range defined by regulation (so that effects on customers would be comparable with those occurring today due to the variability of gas supply), the volumetric flow at the offtakes has to be increased in order to get the same energy. This is caused by the lower volumetric energy content of the hydrogen-diluted natural gas and it impacts on pipe sizing, gas metering and system operation. The analysis also shows potential issues related to the continuous variability of the gas composition that should be faced by the control system. Considering the case study, the initial period of injection yields a ramp of about $0.3\%_{H2}$/min (about 0.08 MJ/Sm^3/min), while composition gradients during injection period are in the order of $0.07\%_{H2}$/min (about 0.018 MJ/Sm^3/min).

Further work will address the quality tracking in a more complex meshed network, considering the transported and delivered energy as a relevant parameter, aiming to further improve the description of real gas transport infrastructures under the new operating regime caused by alternative fuels injection. At the same time, a long-term evaluation of the errors caused in the flow rate measures will be performed, in order to assess the changes that the setting of the metering systems may need.

References

[1] European Commission. Energy roadmap 2050. COM/2011/0885; 2011.
[2] IEA (International Energy Agency). World energy outlook 2012. Paris, France: OECD/IEA; 2012.
[3] IEA (International Energy Agency). ETP – Energy technology perspectives 2012. Paris, France: OECD/IEA; 2012.
[4] IEA (International Energy Agency). Technology roadmap – Bioenergy for heat and power. Paris, France: OECD/IEA; 2012.
[5] Bull A. Biomethane regions EU project – final report; 2014. <www.biomethaneregions.eu/> [Accessed: 31-Aug-2015].
[6] van Foreest F. Perspectives for biogas in Europe; 2012. <http://www.oxfordenergy.org/wpcms/wp-content/uploads/2012/12/NG-70.pdf> [Accessed: 31-Aug-2015].
[7] IEA (International Energy Agency). Harnessing variable renewables: a guide to the balancing challenge. Paris, France: OECD/IEA; 2011.
[8] Guandalini G, Campanari S, Romano MC. Power-to-gas plants and gas turbines for improved wind energy dispatchability: energy and economic assessment. Appl Energy 2015;147:117–30.
[9] Lehner M, Tichler R, Steinmueller H, Koppe M. Power-to-gas: technology and business models. Springer; 2014.
[10] IEA (International Energy Agency). Gas medium-term market report 2012. Paris, France: OECD/IEA; 2012. p. 2012.
[11] TERNA. Statistical data; 2015. <http://www.terna.it/default/home_en/electric_system/statistical_data.aspx>. [Accessed: 09-Apr-2015].
[12] Ríos-Mercado RZ, Borraz-Sánchez C. Optimization problems in natural gas transportation systems: a state-of-the-art review. Appl Energy 2015;147:536–55.
[13] Chertkov M, Backhaus S, Lebedev V. Cascading of fluctuations in interdependent energy infrastructures: gas-grid coupling. Appl Energy 2015;160:541–51.
[14] Matko D, Geiger G, Gregoritza W. Pipeline simulation techniques. Math Comput Simul 2000;52(3–4):211–30.
[15] Aalto H. Transfer functions for natural gas pipeline systems. In: Proceedings of the IFAC 17th world congress, no. 1; 2008. p. 889–94.
[16] Herrán-González A, De La Cruz JM, De Andrés-Toro B, Risco-Martín JL. Modeling and simulation of a gas distribution pipeline network. Appl Math Model 2009;33(3):1584–600.
[17] Osiadacz A, Chaczykowski M. Comparison of isothermal and non-isothermal pipeline gas flow models. Chem Eng J 2001;81(1–3):41–51.
[18] Glaister P. Real gas flows in a duct. Comput Math Appl 1992;24(11):45–59.
[19] Ke SL, Ti HC. Transient analysis of isothermal gas flow in pipeline network. Chem Eng J 2000;76(2):169–77.
[20] Schmidt M, Steinbach MC, Willert BM. High detail stationary optimization models for gas networks. Optim Eng 2015;16(1):131–64.
[21] Mischner J. Notices about hydraulic calculations of gas pipelines. GFW/Gas Erdgas 2012;4:158–273.
[22] ISO. UNI EN ISO 6976:2008 – natural gas – calculation of calorific values, density, relative density and Wobbe indices from composition; 2008.
[23] GERG. Standard GERG virial equation for field use; 1991.
[24] NIST (National Institute of Standards and Technology). NIST reference fluid thermodynamic and transport properties – REFPROP 9.1; 2013. <www.nist.gov>.
[25] Shampine LF, Reichelt MW. The matlab ode suite. SIAM J Sci Comput 1997;18:1–22.
[26] SIMONE – Solutions for simulation and optimisation in the gas industry. <www.simone.eu>.
[27] Liwacom. SIMONE software – Equations and methods; 2004.
[28] Gahleitner G. Hydrogen from renewable electricity: an international review of power-to-gas pilot plants for stationary applications. Int J Hydrogen Energy 2013;38(5):2039–61.

[29] E.ON. E.ON power-to-gas pilot unit in Falkenhagen; 2014. <http://www.eon.com/en/media/news/press-releases/2014/9/1/eon-power-to-gas-pilot-unit-falkenhagen.html> [Accessed: 01-Jan-2015].

[30] GRIDGAS project. <http://www.gridgas.co.uk/> [Accessed: 01-Jan-2015].

[31] Iskov H, Rasmussen N. Global screening of projects and technologies for power-to-gas and bio-SNG. Horsholm: Danish Gas Technology Centre; 2013. 739-27.

[32] Altfeld K, Pinchbeck D. Admissible hydrogen concentrations in natural gas systems. Gas Energy 2013;3:12.

[33] NATURALHY European Project (FP6). Preparing for the hydrogen economy by using the existing natural gas system as a catalyst – final report. SES6/CT/2004/502661; 2010.

[34] SNAM S.p.A. Codice di rete SNAM Rete Gas S.p.A. (Grid code) [Italian language]; 2014.

[35] Guandalini G, Campanari S. Wind power plant and power-to-gas system coupled with natural gas grid infrastructure: techno-economic optimization of operation. In: Proceedings of ASME Turbo Expo 2015, GT2015-42229, June 15–19 2015, Montréal, Canada.